Published by :
http://www.ijert.org

International Journal of Engineering Research & Technology (IJERT)
ISSN: 2278-0181
Vol. 5 Issue 03, March-2016

Modification in Structural, Electrical and Magnetic Properties of Pr Doped Bismuth Ferrites

Anu Beniwal[1], Jarnail S. Bangruwa[1], Balesh Vasisth[1,2], S. P. Gairola[2], Vivek Verma[1]
[1]Department of Physics, Hindu College, University of Delhi, Delhi, India
[2]Department of Physics, Uttaranchal University, Dehradun, India

***Abstract* - Pure and Pr doped multiferroic samples of bismuth ferrites (BFO) were successfully synthesized by the sol-gel technique. Detailed investigations were made on the influence of Pr on structural, electrical, ferroelectric and magnetic properties of the BFO. The XRD patterns confirm the formation of pure phase, rhombohedral structure in BFO. It is also observed that Pr-doping increases the symmetry and decreases the second phases noticeably. Microstructure investigation using the scanning electron microscope showed a reduction of grain size with doping in BFO. Magnetic hysteresis loops showed that retentivity (Mr), coercivity (Hc) and saturation magnetization (Ms) of the doped samples were improved. Furthermore, the Pr-doping enhances the dielectric properties as a result of the reduction in the Fe^{2+} ions and oxygen vacancies. The room temperature P-E loop study shows that ferroelectric properties are strongly depend on doping.**

Keywords: Multiferroic; Ferrites; Sol-gel; Structural; Magnetic; Dielectric; Ferroelectric

1. INTRODUCTION

The coexistence of ferroelectricity and magnetic nature in a single material is known as multiferroics, gives an additional degree of freedom to design various unconventional devices, such as multistate memory elements and electric-field controlled magnetic sensors. However, the simultaneous interaction of various electric orders parameters in a given system also posses new challenge for fundamental physics. The key to device functionality is a multiferroic material with strong magnetoelectric (ME) coupling for making a control of magnetization via polarization and vice versa. Unfortunately, very few materials have shown coexistence of ferroelectricity and magnetization at room temperature [1-3]. $BiFeO_3$ (BFO) is the only single phase material which shows multiferroic phenomenon at room temperature having relatively high ferroelectric Curie temperature (Tc ~ 1103 K) and antiferromagnetic Neel temperature (T_N ~ 643 K) and among the all identified single-phase magnetoelectric multiferroics, BFO exhibits the large polarization value [4-6]. Coupling between the electrical and magnetic order, multiferroic can provide an extra degree of freedom in design of new functional sensor and multistate memory devices [7, 8]. BFO exhibits rhombohedrally distorted perovskite (ABO_3) crystal structure with R3c space group. It exhibits G-type antiferromagnetism due to the local spin ordering of Fe^{3+} which forms a cycloidal spiral spin structure having spin periodicity of 62 nm [9]. The magnetic moment of ions rotate along the propagation direction of the modulated wave in the plane perpendicular to the hexagonal basal plane. The modulation inhibits the observation of week ferromagnetism and of linear magnetoelectric effect [10]. Due to the existence of Fe^{2+} and oxygen vacancies, BFO suffers from large leakage current, which limits the applications of BFO. The site-engineering concept has been widely explored in an effort to reduce the current leakage, improve the ferroelectric behaviour, and enhance the magnetoelectric coupling in BFO [8]. Recently, the multiferroic properties of BFO can be highly enhanced by doping with rare-earth or transition metal either at A-site, or B-site, or A-B-site [11, 12]. Several research groups have reported that the superior ferroelectric property can be obtained through reduction of leakage current due to suppression oxygen vacancies with single doping or co-doping. Assuredly, some element doping such as Tb, Pr, Nd, Ru, Sr and Sm at A-site (Bi-site) can effectively reduce the impurity phases, the formation of defects and the chemical fluctuation [13-15]. The Doped elements also influence spatially modulation spiral spin structure of BFO and in this way small improvement in the magnetic properties can be achieved. There are many reports on the doping of transition metal ions such as Co, Cr, Ti, Mn, Zn etc. at B-site (Fe-site) in BFO with the enhance magnetoelectric properties [16, 17]. It is observed that the electrical properties of BFO ceramics improved by doping of trivalent La^{3+} and other dopants at Bi^{3+} site. Simoes et al. [18] and Wang et al. [19] suggested that La^{3+} doping in BFO effectively reduce the concentration of charge defects and dielectric losses. It is, therefore, clear that rare-earth ion doping at B-site in BFO compound is worthwhile in observing the improved properties as compare to undoped BFO. In recent years, some studies on the multiferroic properties of Pr-doped BFO have been reported, where Pr^{3+} doping has been explored for reducing oxygen vacancies in BFO ceramics due to the Pr-O bond been stronger than the Bi-O bond [12]. However, no detailed reports are available in the literature on the magnetic, electrical and dielectric properties of Pr-doped BFO ceramics so far. In this paper, the strategy of Pr doping was adopted for the enhanced ferroelectric and magnetic properties in BFO. Pr ions were introduced in A-site of BFO, and attempt to a systematic study on structural, dielectric, electric polarization and magnetic properties of doped bismuth ferrites.

International Journal of Engineering Research & Technology (IJERT)
ISSN: 2278-0181
Vol. 5 Issue 03, March-2016

2. EXPERIMENTAL

In recent years, the sol-gel technique has emerged as a versatile method for synthesizing different inorganic materials. Apart from the advantage of low temperature synthesis a sol-gel route make it possible to obtain pure phase materials. Pure and doped $Bi_{1-x}Pr_xFeO_3$ samples where $0 \leq x \geq 0.20$ in step of 0.1 namely, $BiFeO_3$ (BFO), $Bi_{0.9}Pr_{0.1}FeO_3$ (BFO1), $Bi_{0.8}Pr_{0.2}FeO_3$ (BFO2), were successfully synthesized by the sol-gel technique. The precursor solutions were prepared by using highly pure $Bi(NO_3)_3.5H_2O$, $Fe(NO_3)_3.9H_2O$, $Pr(NO_3)_3.6H_2O$ as the starting materials and distilled water as a solvent. The stoichiometric ratio of these materials were dissolved in the distilled water and HNO_3 to form the aqueous solutions. Citric acid was subsequently added as a complexing agent in an appropriate proportion to the above solution under constant stirring. The resultant solution was then evaporated and dried at approximately 80°C on a hot plate under continuous stirring to obtain xerogel powders. Then the xerogel powders were grinded in the agate mortar. The obtained powder samples were annealed at 600°C for 4h in order to obtain the pure phase. The well dense pallets of different samples were obtained by applying hydraulic pressure of 10 ton for the well grinded powder mixed with PVA solution and subsequently sintered at 650 ^{0}C for half four hours. Both sides of pallets were polished with silver paste for electric characterization. The initial investigation of structural and microstructure analysis was carried out by Philips X'Pert X-ray diffractometer using CuKα radiation with wavelength 1.5406 Å. The room temperature magnetic measurements were performed with vibrating sample magnetometer (EV-9, Microsense). The morphology of samples was characterized by Scanning Electron Microscopy (FEI, QUANTA 200F). The dielectric measurements were performed with the help of Precision 6500B Impedance Analyzer. The ferroelectric were carried out using the Automatic P–E Loop Tracer (Marine India).

3. RESULTS AND DISCUSSIONS

The XRD patterns for pure and Pr-doped BFO samples are shown in Figure 1. Pure sample show few impurity peaks (marked by * in Figure 1) of Bi_2FeO_9 ($2\theta = 27.6^{\circ}$) and $Bi_{36}Fe_2O_{57}$ ($2\theta = 32.8^{\circ}$), while no impurity peaks are observed for compositions of x = 0.1 and 0.2, which indicates that Pr doping in BFO at A-site is helpful in reducing the secondary phases. The occurrence of secondary phases is generally observed in pure BFO due to the kinetics of phase formation and high volatility of bismuth. The crystal structure of the pristine sample shows the distorted pervoskite structure with rhombohedral lattice type and R3c space group.

All the XRD patterns demonstrate that the sharp peaks correspond to the diffraction from (012), (014), (110), (006), (202), (116), (122), (018) and (214) planes of the rhombohedral structure of BFO. With increasing Pr concentration in BFO, the XRD pattern is observed to shift towards higher 2θ value as shown in Figure 1(b). This shift in the XRD patterns indicates that the dopants get substituted in the BFO lattice. Also, the separated peaks corresponding to the planes (104) and (110); (006) and (202) around 2θ values range of ~ 31.4º-32.4º, 38.7º-39.7º respectively, are tending to merge in to one broadened peak, for doped samples. However, it can be seen that the peaks are still split in accordance with the rhombohedral distortion but the splitting degree is reduced in consistence with reduced rotation angle, which indicates that the rhombohedral distortion reduces toward to orthorhombic by Pr doping, but it does not change into orthorhombic completely. The similar kind of phase transformation behaviour was also observed in La-doped $BiFeO_3$ ceramics by Cheng et al [20]. Thus, the undertaken structural investigation of $Bi_{1-x}Pr_xFeO_3$ system revealed a sequence of the substitution-driven first-order phase transition.

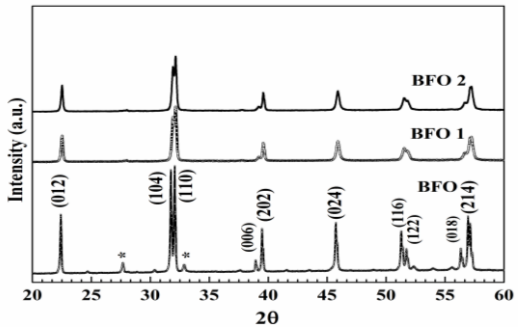

(a)

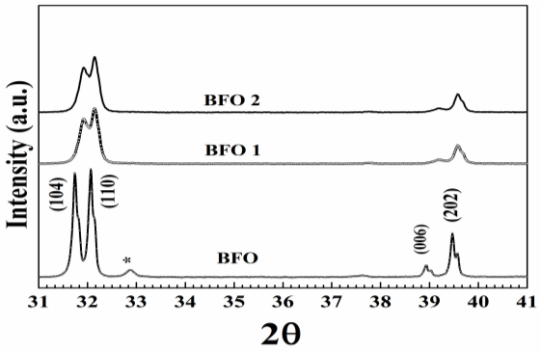

(b)

Figure 1. XRD pattern of pristine and doped BFO samples (a) 2θ = 20° – 60° and (b) 2θ = 31° - 41°.

Figure 2. shows the scanning electron micrograph (SEM) of pure and doped BFO samples. The morphology of the samples is dense and uniform. All the samples have clear and small grains as well as grain boundaries. Grain sizes of doped samples were found to decrease with doping. The decreased aspect ratio of the grains improves the density of the samples (resulting in the high resistivity of the samples). It means that Pr doping can suppress grain growth and lead to small grain sizes in the materials as we can observe from SEM of BFO2 sample. The decrease in grain size may be attributed to the difference in the ionic radius of Bi^{3+} and Pr^{3+}. Kirkendall effect may be the another reason for reduction in grain size due to doping which arise due to diffusion rates of constituting elements of the compounds. It is also noted from the literature that

International Journal of Engineering Research & Technology (IJERT)
ISSN: 2278-0181
Vol. 5 Issue 03, March-2016

the decrease in the grain size is attributed to the suppressed oxygen vacancies as a result of Pr doping, since it is the oxygen vacancies motion during the sintering process which facilitates the grain growth [21].

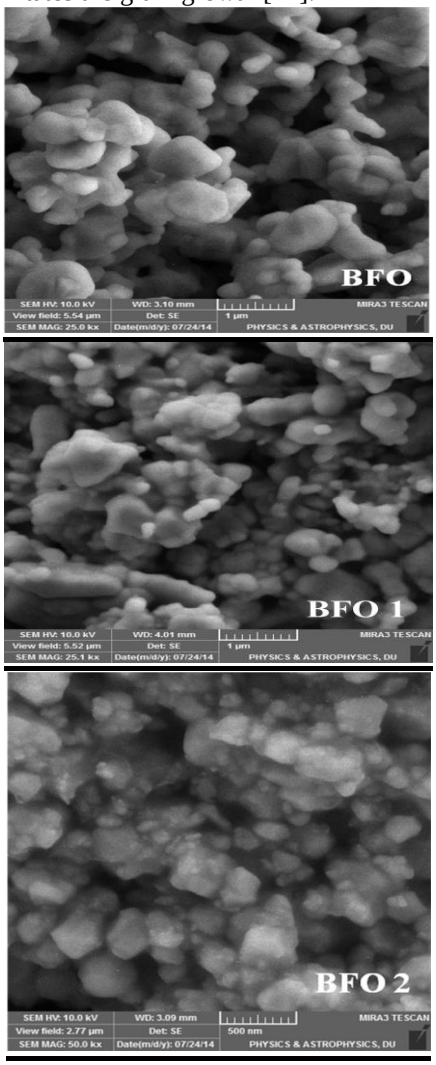

Figure 2. SEM micrographs for pristine and doped BFO samples.

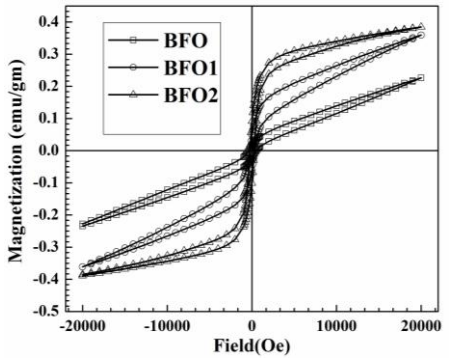

Figure 3. M-H loops for pristine and doped BFO samples

Figure 3. shows the M-H loops for pure and doped bismuth ferrites at room temperature. Parameters such as saturation magnetization and coercivity were determined from the M-H curves. All the samples show magnetic hysteresis loops representing weak ferromagnetic (FM) behaviour. The parent compound (BFO) is reported to G-type antiferromagnetic due to local spin ordering of Fe^{3+} at room temperature. The M-H loops show a magnetization of 0.22 emu/g for BFO sample and no tendency to saturate up to the maximum applied field of 2T. We obtained a remnant magnetization 2Mr = 0.042 emu/g and coercivity of 2Hc = 964 Oe for BFO sample. With Pr doping magnetization increases to 0.39 emu/g, remnant magnetization 2Mr = 0.196 emu/g and coercivity decreases to 2Hc = 500 Oe for BFO2 sample. It is clear that Pr doping plays the dominant role towards the increase in the magnetization of BFO samples. At the same time, there are several reports that show the FM like magnetic hysteresis in pure BFO compound. It is, therefore, questionable whether the room temperature weak FM character is intrinsic or extrinsic magnetic property of BFO. It may arises due to impurities of γ-Fe_3O_4 of Fe_3O_4. Since the observed coercivity for γ-Fe_3O_4 and Fe_3O_4 are 450 Oe and 25 Oe respectively. In the present study, the observed coercivity of BFO is about 482 Oe, which differ those of γ-Fe_3O_4 and Fe_3O_4 ruling out their presence as secondary phase. The other possibility is the presence of the $Bi_{25}FeO_{39}$ phase which can be confirmed by the XRD pattern. With Pr doping in BSFO sample the $Bi_{25}FeO_{39}$ impurity phase gets suppressed and as a result of this the coercivity and remnant magnetization decreased substantially. The XRD results reveald that Pr doping improve the phase formation of bismuth ferrites. In BFO, Fe^{3+} ion is surrounded by the six O^{2-} ions and O^{2-} ion is the common apex of two adjacent FeO_6 octahedra. The ionic size of Bi^{3+} is larger than that of substituted Pr^{3+} ions. Substitution of smaller ionic size elements, at Bi^{3+}-site, decreases the average A-site ionic size which in turn decreases tolerance factor. This, in-turn increase the octahedral tilt and change in the Fe-O-Fe bond angle and Fe-O bond distances which affacts the superexchange interaction between the two antiferromagnetically aligned Fe^{3+}-ions with possibility of canted structure which in turn an enhancement in ferromagnetic nature of the samples [22]. Therefore, 3d moments of Fe^{3+} ions align ferromagnetically with the 4f spin-moment of the Pr^{3+} ions and ferromagnetic exchange interaction between the Pr^{3+} and Fe^{3+} magnetic ions improve the magnetization in BFO1 and BFO2 samples. Though the M-H curves show non-linear behavior but magnetization curves do not exhibit any tendency to saturate even at 2T, which may be due to the uncompesated antiferromagnetic nature persisting in the samples.

International Journal of Engineering Research & Technology (IJERT)
ISSN: 2278-0181
Vol. 5 Issue 03, March-2016

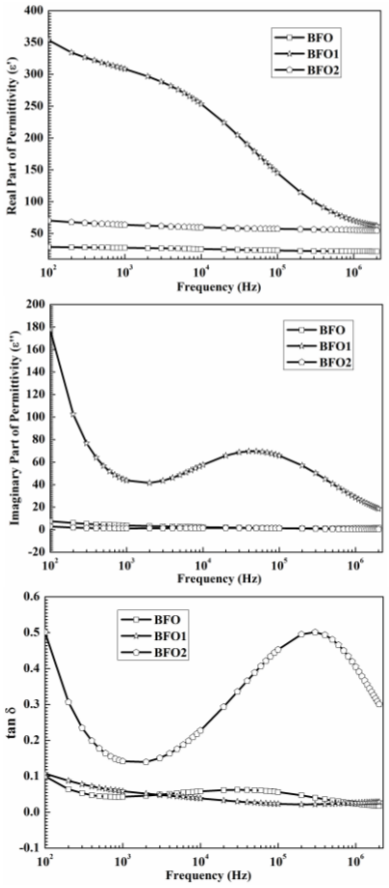

Figure 4. Variation of dielectric constant and loss tangent with frequency for pristine and doped BFO samples.

Frequency dependent dielectric properties of pure and doped BFO samples were measured at room temperature in the frequency range of 100 Hz to 1 MHz as shown in Figure 4. It is observed that real part of dielectric (ε')is decreased rapidly by increasing frequency and become independent at high frequencies. The decrement in ε' is attributed to the dielectric relaxation. The dielectric desperson can be explained by Koop's theory. According to this theory the decrement in ε' with increasing frequency is assigned to the fact that atoms in the dielectric material need a finite time to align up their axis in the applied field direction. As the frequency of the electric field increases, a point is reached when charge carriers of dielectric do not follow with the frequency of the applied electric field and value of ε' is decreased. With further increase in the frequency of the applied field, at last, the polarization would hardly have started to move before the field reverses and makes no contribution to polarization and so ε' become independent at high frequencies. Another very important point of the decrement in dielectric constant is related with the hopping of the electrons from Fe^{2+} to Fe^{3+} ions. At low frequency, flectric field does not provide enough energy to electron for hopping but as we increase the frequency of electric field then it provides sufficient energy and a point is reached when hopping of electron is started from Fe^{2+} to Fe^{3+} ions. Therefore, the conductivity of the dielectric increases as frequency is increased and hence a decrement occure in ε' [23].

On doping with Pr the value of dielectric constant increases. At a frequency of 1kHz the value of the dielectric constant for BFO sample is 27.6 which increases to 308.3 for BFO1 and 63.76 for BFO2 sample. BFO2 sample shows a very low dielectric dispersion similar behavior to undoped BFO. Percentage increase of dielectric constant (ε′) and loss(ε′′) from 2MHz to 100Hz is 28.7% and 382% in case of BFO2 sample and for BFO1 it is 469.4% and 849.6% respectively. For undoped BFO, it is 32% and 671.4% respectively. Intrinsic value of dielectric constant which is generally the value at high frequency is also high in case of Pr doped samples. At 2MHz the value of dielectric constant for BFO1 and BFO2 samples are 62.09 and 54.76 respectively. In comparison the value for undoped BFO sample is 21.88. The increase in the value of intrinsic dielectric constant indicates that the Pr doping produces major structural changes in the crystalline structure of BFO and is well suggested by the X-ray diffraction patterns.

However, the two different doping concentrations of Pr are quite different in the dielectric behavior. While BFO1 sample show some type of relaxation behavior as indicated by the peak in the dielectric loss, BFO2 sample show a similar behavior to undoped BFO as a low loss material with flat loss. In fact the dielectric dispersion in BFO2 sample is even less than undoped BFO (increase of dielectric constant (ε′) and loss(ε′′) from 2MHz to 100Hz is 28.7% and 382% in case of BFO2 sample and for undoped BFO it is 32% and 671.4% respectively). The very low dielectric dispersion in BFO2 samples also indicate that the space charge contribution due to oxygen vacancies is also reduced leading to reduced dc conductivity as confirmed by the grain size in SEM photographs.

Figure 5 shows the ferroelectric hysteresis loop measured for pure and doped BFO at room temperature. All samples show a linear loosy and unsaturated loop. With Pr doping, there is an increase in observed saturation polarization (P_s), remnant polarization (P_r) and coercive field (E_c). The remanent polarization of BFO2 is 4.5 $\mu C/cm^2$, which is much larger that that of BFO (2.8 $\mu C/cm^2$) sample. The improved ferroelectric property may aries from the changes of Bi-O bonds with Pr doping because the ferroelectric of BFO originates from the stereochemical activity of Bi lone pairs [24].

International Journal of Engineering Research & Technology (IJERT)
ISSN: 2278-0181
Vol. 5 Issue 03, March-2016

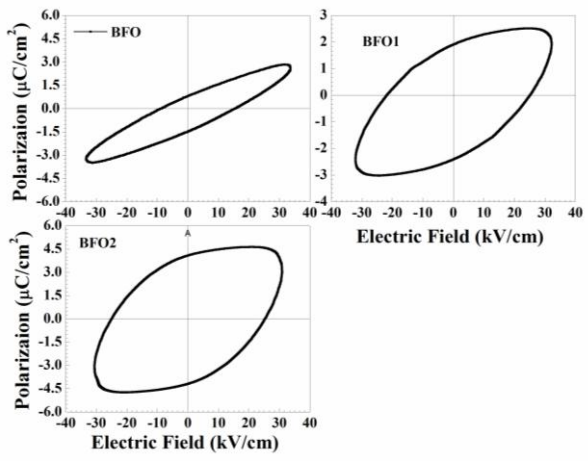

Figure 5. Ferroelectric hysteresis loops for pristine and doped BFO samples at room temperature.

3.5 Conclusions

$Bi_{1-x}Pr_xFeO_3$ samples are synthesized using sol-gel method for pure phase formation. The XRD analysis revealed that all these samples exist in rhombohedral structure. An enhancement in ferromagnetic nature of the samples was observed due to Pr doping. It is observed that real part of dielectric constant (ε′) decreases with the increase in frequency and the high value of dielectric constant at low frequency (less than 1 kHz) as observed for the samples due to dielectric relaxation. Compared BFO with BFO1 and BFO2 samples, the ferroelectric properties are effectively enhanced with Pr doping.

3.6 Acknowledgements

The authors are grateful to Department of Science and Technology (DST) for providing Fast Track Young Scientist Project SR/FTP/PS-161/2011 to carry out this work. The authors are grateful to Principal, Hindu College and University of Delhi (USIC) for constant encouragement and measurement facilities.

REFERENCES

[1.] W. Eerenstein, N. D. Mathur and J. F. Scott, Nature (London) **442**, 759 (2006).
[2.] J. M. Caicedo, J. A. Zapata, M. E. Gomez and P. Prieto, J. Appl. Phys. **103**, 07E306 (2008).
[3.] N. A. Hill, J. Phys. Chem. B **104**, 6694 (2000).
[4.] J. Wang, J. B. Neaton, H. Zheng, V. Nagrajan, S. B. Ogale and B. Liu, Science **299**, 1719 (2003).
[5.] G. Catalan, J. F. Scoot, Adv. Mater. **21**, 2463 (2009).
[6.] G. S. Arya, R. K. Sharma, N. S. Negi, Mater. Lett. **93**, 341-4 (2013).
[7.] K. Takahashi, n. Kida, M. Tonouchi, Phys. Rev. Lett. **96**, 117402 (2006).
[8.] G. Dong, G. Tan, Y. Luo, W. Liu, H. Ren and A. Xia, Appl. Surface Scie. **290**, 280-286 (2014).
[9.] I. Sosnowska, T.P. Neumaier and E. Steichele, J. Phys. C **15**, 4835 (1982).
[10.] C. Ederer and N. A. Spaldin, Phys. Rev. B **71**, 060401 (2005).
[11.] S. U. Lee, S. S. Kim, M. H. Park, J. W. Kim, H. K. Jo and W. J. Kim, Appl. Surf. Sci. **254**, 1493 (2007).
[12.] I. Coondoo, N. Panwar, I. Bdikin, V. S. Puli, R. S. Katiyar and A. L. Kholkin, J. Phys. D **45**, 055302 (2012).
[13.] Y. Wang and C. W. Nan, J. Appl. Phys. **103**, 024103 (2008).
[14.] S. K. Singh, Thin Solid Films **527**, 126 (2013).
[15.] F. Yan, M. O. Lai and L. Lu, J. Phys. Chem. C **114**, 6994 (2010).
[16.] H. R. Yan, H. M. Deng, N. F. Ding, J. He, L. Peng, L. Sun, Mater. Lett. **111**, 123 (2013).
[17.] H. Naganuma, J. Miura and S. Okamura, Appl. Phys. Lett. **93**, 052901 (2008).
[18.] A. Z. Simoes, F. G. Garcia, and C. D. S. Riccardi, J. Mater. Chem. Phys. **116**, 305 (2009).
[19.] Y. Wang, R. Y. Zheng, C. H. Sim, and J. Wang, J. Appl. Phys. **105**, 016106 (2009).]
[20]. Z. X. Cheng, A. H. Li, X. L. Wang, S. X. Dou, K. Ozawa, H. Kimura, S. J. Zhang, and T. R. Shrout, J. Appl. Phys. **103**, 07E507 (2008).
[21.] Prachi Sharma, Vivek Verma, J. Mag. Mag. Mater.**374,** 18–21(2015).
[22.] Virendra Kumar, Anurag Gaur, Neha Sharma, Jyoti Shah and R. K. Kotnala, ceramics International **39**, 8113-8121 (2013).
[23.] Aparna Saxena, Prachi Sharma, Anjali Saxena, Vivek Verma, Raghvendra Sahai Saxena, Ceramics International **40**,15065–15072 (2014) .
[24.] Weiwei Mao,, Xingfu Wang, Yumin Han, Xing'ao Li, Yongtao Li, Yufeng Wang, Yanwen M,Xiaomiao Feng, Tao Yang, Jianping Yang, Wei Huang, J.Alloys and Comp. **584**, 520–523 (2014) .